

What a difference a quadrupole makes?

Daniele Malafarina* and Sabina Sagynbayeva†

Department of Physics, Nazarbayev University, 010000 Nur-Sultan, Kazakhstan

We consider some implications of the departure from spherical symmetry for solutions of the vacuum Einstein's equations describing black hole mimickers. In particular, we investigate how the presence of quadrupole moment affects the collision energy of test particles. We show that collision processes in the vicinity of such exotic compact sources with quadrupole moment may be significantly different from those in the vicinity of black holes. Particles can not cross the infinitely red-shifted surface $r = 2M$ with the exception of the special case of spherical symmetry. Also we show that the center of mass energy for particle collisions diverges at $r = 2M$ for prolate sources while it is finite for oblate sources.

PACS numbers: 04.20.Dw, 04.20.Jb, 04.70.Bw

I. INTRODUCTION

The No-Hair Theorem (NHT) states that asymptotically flat black hole solutions in General Relativity (GR) are fully characterized by three quantities only, namely mass, angular momentum and charge [1, 2]. These black hole solutions are: (i) Schwarzschild, describing static, uncharged black holes, (ii) Kerr, describing stationary, uncharged black holes, (iii) Reissner-Nordstrom, describing static, charged black holes and (iv) Kerr-Newman, describing stationary, charged black holes. The validity of the NHT relies on the space-time being asymptotically flat and vacuum. Of course, the assumptions that go in the no hair theorem are not perfectly realized in nature. In particular, real astrophysical objects are not in perfect vacuum and need not necessarily obey the symmetry of the Kerr space-time. This leads to the natural question of how to interpret the theorem in the context of more realistic astrophysical situations (see for example [3, 4]). To what extent can we then rely on the NHT to describe astrophysical black holes? And what are the consequences of the departure from the black hole space-times for extreme astrophysical compact objects? Do slight departures from a black hole line element lead to slight modifications in the observable features of the geometry? Or, on the contrary, do they lead to significant differences?

To investigate such questions it is worth considering the consequences of relaxing the symmetry requirements of the space-time. As it is well known, asymptotically flat vacuum and static solutions outside of spherical symmetry in general describe the gravitational field in the exterior of non spherical objects [5]. Also, it is well known that there exist an infinite number of solutions of Einstein's equations describing stationary and vacuum space-times which are not black holes. In particular, restricting the attention to static and axially symmetric sources, the so called Weyl class [6, 7], there exist a one-to-one correspondence between solutions of Laplace equation in flat two-dimensional space and static, axially symmetric solutions of the four-dimensional vacuum field equations [8, 9]. The question is then, what happens when such objects collapse indefinitely under their own gravity. Since solutions belonging to Weyl's class, with the exception of Schwarzschild, possess curvature singularities at the location of the infinitely red-shifted surface (in Schwarzschild coordinates $r = 2M$), we can envision two possible scenarios:

- (i) All higher multipole moments are radiated away via gravitational waves during collapse and the space-time settles to the Schwarzschild geometry. In this case the horizon can be treated as a purely classical entity and the breakdown of the relativistic description occurs as the curvature diverges, i.e. in the vicinity of the central singularity at $r = 0$.
- (ii) The collapsing object retains some of the higher multipole moments as the infalling matter approaches the surface $r = 2M$. The horizon does not form and either matter is dispersed away or an exotic compact object forms. In this case, the curvature singularity appearing in non spherical solutions must be treated as a quantum-gravitational object and it signals the breakdown of general relativity in its vicinity.

In case (i) we face the usual problems related to the formation of singularities as the endstate of collapse [10, 11] such as, for example, the information loss paradox [12]. In particular, it appears that the resolution of such singularities must entail non local effects that affect the geometry in the horizon region of the space-time, even if such horizon has low curvature and may be located far from the quantum-gravity dominated region (see [13] for a review). In case (ii) we are also faced with the existence of singularities, however the interpretation of such singularities is more straightforward and their eventual resolution may not lead to the problems mentioned above. In fact, in this case we may consider that the limits of applicability of the classical theory

*Electronic address: daniele.malafarina@nu.edu.kz

†Electronic address: sabina.sagynbayeva@nu.edu.kz

are reached already near the horizon, i.e. when $2GM/(c^2r) \simeq 1$. Massive particles do not cross the null divide and a quantum treatment is necessary already at the horizon level.

In the following we will explore the alternative point of view (ii) assuming that not all higher multipole structure is radiated away during collapse and therefore the final object forming from complete collapse will not be spherically symmetric. Therefore we will assume that a Weyl line element can describe an extremely collapsed object which need not be a black hole in a strict mathematical sense. However, due to the slight departures from spherical symmetry, such an object may mimic the appearance of a black hole for certain kinds of observations. In this perspective, we wish to investigate the effects that the presence of quadrupole moment has on the appearance of the black hole mimicker. To this aim we will focus on two of the most important line-elements belonging to Weyl's class with non vanishing quadrupole moment, namely the Erez-Rosen (ER) metric [14–18] and the Zipoy-Voorhees (ZV) metric [19–22]. Since in both cases the surface $r = 2M$ in Schwarzschild-like coordinates has infinite redshift, the object may still appear like a black hole for certain observations, and may be labeled as a black hole mimicker. However, other kinds of observations may allow to distinguish the geometry from Schwarzschild and Kerr (see for example [23–28]). In this work, we will concentrate the attention on the effect that the quadrupole moment has on the center of mass energy for the collision of test particles in the vicinity of the compact object. Collisions of test particles in the geometry of extreme compact objects was brought to prominence by Banados, Silk and West who considered the Schwarzschild and Kerr cases [32]. Since then, many studies have been carried out to understand the mechanism of energy collisions near compact objects and its possible implications for astrophysics (see for example [33–38]).

The paper is organised as follows: In section II we will briefly review static axially symmetric vacuum solutions of Einstein's equations with particular attention to two important solutions with quadrupole moment, namely the ER and the ZV solutions. In section III we will explore particle collisions in these space-times to investigate how they depart from the corresponding scenarios in the Schwarzschild geometry. Finally in section IV we will discuss the implications that can be drawn for the physical validity of non black hole space-times as describing astrophysical compact objects. In the following we make use of geometrized units setting $G = c = 1$.

II. STATIC AXIALLY SYMMETRIC VACUUM SOLUTIONS

The class of vacuum, static and axially symmetric space-times takes the name of Weyl class [6] and the most general line element in Schwarzschild-like coordinates $\{t, r, \theta, \phi\}$ can be written as

$$ds^2 = -F(r, \theta)dt^2 + \frac{G(r, \theta)}{F(r, \theta)} \left[\frac{\Sigma(r, \theta)}{\Delta(r)} dr^2 + \Sigma(r, \theta)r^2 d\theta^2 \right] + \frac{\Delta(r)}{F(r, \theta)} r^2 \sin^2 \theta d\phi^2, \quad (1)$$

where $F(r, \theta)$ and $G(r, \theta)$ need to be determined from Einstein's equations while

$$\Delta(r) = 1 - \frac{2M}{r}, \quad (2)$$

$$\Sigma(r, \theta) = 1 - \frac{2M}{r} + \frac{M^2}{r^2} \sin^2 \theta. \quad (3)$$

It is well known that there exist a one-to-one correspondence between solutions of Laplace equation in 2-dimensional flat space and solutions belonging to Weyl's class in cylindrical coordinates [8]. Therefore, in principle, $F(r, \theta)$ and $G(r, \theta)$ can be determined once a solution of Laplace equation is given and therefore all exact solutions in the form (1) are known. However, while the physical interpretation of solutions of Laplace equations is straightforward in Newtonian mechanics not the same can be said for their relativistic counterparts. In fact, one may write the solution to Laplace equation in terms of a sum of Legendre polynomials and the coefficients a_n multiplying each polynomial, which are usually called Weyl multipoles, do not correspond to the gravitational multipoles M_n [9]. For example, the Weyl monopole is the Curzon solution [39], while the gravitational monopole is of course the Schwarzschild solution. Therefore the physical interpretation of Weyl's solutions is not straightforward.

One of the most remarkable features of Weyl's solutions is that they generically possess naked singularities. These singularities may have different physical interpretation depending on the corresponding interpretation of the geometry. For example, the naked singularity in the double Schwarzschild solution may be interpreted as strut keeping the two massive sources in place, thus allowing for the solution to be static while in a more physically realistic description it must be dynamical [40].

Here we are interested in the role played by small departures from spherical symmetry in the form of non vanishing quadrupole moment. In this respect the two most interesting solutions are the Erez-Rosen (ER) solution [14], which extends the Schwarzschild solution with the introduction of a non vanishing quadrupole moment while all higher multipole moments vanish, and the Zipoy-Voorhees (ZV) solution [19, 20], also known as γ -metric, which extends the Schwarzschild solution with the introduction of non vanishing even multipole moments of every order, all depending on a single parameter γ . Both solutions present a naked singularity at the surface $r = 2M$, where in the spherical case the horizon is located.

A. Schwarzschild

The Schwarzschild solution is spherically symmetric and is the only asymptotically flat, static and vacuum solution which describes a black hole. It can be obtained from the line element (1) when F and G are given by

$$F(r) = \Delta(r), \quad (4)$$

$$G(r, \theta) = \frac{\Delta(r)}{\Sigma(r, \theta)}. \quad (5)$$

For Schwarzschild's multipole moments we have

$$M_0 = M, \quad (6)$$

$$M_n = 0 \quad \text{for } n \geq 1. \quad (7)$$

As it is well known the surface $r = 2M$ identifies the event horizon and, in Schwarzschild's coordinates, it is a coordinate singularity. The curvature is finite at the horizon and the coordinate singularity can be removed by a suitable change of coordinates. Then trajectories may extend inside the horizon and every particle geodesic entering the same will terminate at the curvature singularity located at $r = 0$.

B. Erez-Rosen

The ER solution is the natural extension of the Schwarzschild metric with the addition of quadrupole moment and it is given by

$$F(r, \theta) = \Delta(r)e^{2q\Psi(r, \theta)}, \quad (8)$$

with

$$\Psi(r, \theta) = \frac{3 \cos^2 \theta - 1}{4} \left[\frac{3r^2 - 6Mr + 2M^2}{2M^2} \ln \left(1 - \frac{2M}{r} \right) + 3 \frac{r - M}{M} \right]. \quad (9)$$

The complete expression for G is [17]

$$G(r, \theta) = \frac{\Delta(r)}{\Sigma(r, \theta)} e^{2q\Phi(r, \theta)}, \quad (10)$$

with

$$\begin{aligned} \Phi(r, \theta) = & -3 + \frac{2+q}{2} \ln \left(\frac{\Delta(r)}{\Sigma(r, \theta)} \right) - \frac{3(r-M)}{2M} \ln \Delta(r) + \frac{9q}{16} \sin^2 \theta \left\{ \left(\frac{r-M}{M} \right)^2 (1 - 9 \cos^2 \theta) + \right. \\ & + 4 \cos^2 \theta - \frac{4}{3} + \left(\frac{r-M}{M} \right) \left[\left(\frac{r-M}{M} \right)^2 (1 - 9 \cos^2 \theta) + 7 \cos^2 \theta - \frac{5}{3} \right] \ln \Delta(r) + \\ & \left. + \left(\frac{r^2 - 2Mr}{4M^2} \right) \left[\left(\frac{r-M}{M} \right)^2 (1 - 9 \cos^2 \theta) - \sin^2 \theta \right] \ln^2 \Delta(r) \right\}. \quad (11) \end{aligned}$$

The monopole and quadrupole moments of the ER solution are

$$M_0 = M, \quad (12)$$

$$M_2 = \frac{2qM^3}{15}. \quad (13)$$

Notice that for the ER solution we have $M_{2n} = 0$ for $n \geq 2$ and for $q = 0$ we retrieve the Schwarzschild line element. Then cases where $q > 0$ (and $q < 0$ respectively) are interpreted as representing the field outside prolate (oblate) sources. The ER metric has a true curvature singularity at $r = 2M$ for $q \neq 0$.

C. Zipoy-Voorhees

The ZV solution, also known as γ -metric, is a ‘natural’ axially symmetric extension of the Schwarzschild solution as it depends on only one extra parameter γ describing the departure from spherical symmetry. The metric functions are given by

$$F(r) = \Delta(r)^\gamma, \quad (14)$$

$$G(r, \theta) = \left(\frac{\Delta(r)}{\Sigma(r, \theta)} \right)^{\gamma^2}, \quad (15)$$

and its monopole and quadrupole moments are

$$M_0 = M\gamma, \quad (16)$$

$$M_2 = (1 - \gamma^2) \frac{\gamma M^3}{3}. \quad (17)$$

Notice that, differently from the ER solution, for the ZV solution we have that all even multiple moments M_{2n} do not vanish if $\gamma \neq 1$. For $\gamma = 1$ the line element reduces to Schwarzschild and cases where $\gamma > 1$ (and $\gamma < 1$ respectively) are interpreted as representing the field outside oblate (prolate) sources. Similarly to the ER metric, the ZV metric also has a true curvature singularity at $r = 2M$ for $\gamma \neq 1$.

Note that other solutions characterized by the presence of quadrupole moment do exist. The structure of multipole moments of Weyl’s solutions was extensively studied in [9] with the aim of characterizing solutions based on the properties of the source. Other notable solutions with quadrupole moment were studied for example in [29] and [30] and the role played by quadrupole moment in the motion of test particles was first considered in [31].

III. PARTICLE COLLISIONS

To describe the process of energetic collisions of two test particles of masses m_1 and m_2 in an axially symmetric space-time we follow the framework outlined by Banados, Silk and West in [32]. The 4-velocity of each particle is given by $u_i^\mu = \{\dot{t}_i, \dot{r}_i, \dot{\theta}_i, \dot{\phi}_i\}$, where $i = 1, 2$ and the dot represents derivatives with respect to the proper time τ parametrizing the particle’s trajectory. In the following we will restrict the attention to motion in the equatorial plane, thus setting $\theta = \pi/2$ and $\dot{\theta} = 0$.

Given the symmetry of the space-time we know that there exist two Killing vectors, one related to time translations and one related to rotations about the symmetry axis, which correspond to two conserved quantities, namely the energy of the test particle E and the component of its angular momentum along the direction of the symmetry axis L . Therefore, for each particle, omitting the subscript identifying the particle, from the line element (1) we have

$$\dot{t} = \frac{E}{F}, \quad (18)$$

$$\dot{\phi} = \frac{F L}{\Delta r^2}, \quad (19)$$

and the 4-velocity of the test particle in the equatorial plane becomes $u^\mu = \{E/F, \dot{r}, 0, (FL)/(\Delta r^2)\}$. Then we can write

$$p_\mu p^\mu = -m^2 = -\frac{E^2}{F} + \frac{G\Sigma}{F\Delta} \dot{r}^2 + \frac{F L^2}{\Delta r^2}. \quad (20)$$

which can be used to obtain \dot{r}^2 . The center of mass energy E_{cm} for two colliding particles is given in general by

$$E_{\text{cm}}^2 = m_1^2 + m_2^2 - 2g_{\mu\nu} p_1^\mu p_2^\nu, \quad (21)$$

where $p_i^\mu = m_i u_i^\mu$ (with $i = 1, 2$) is the particle’s 4-momentum. In the following, for the sake of clarity, we will consider particles with the same mass $m_1 = m_2 = m$ that have zero radial velocity at spatial infinity. Taking $\dot{r} \rightarrow 0$ for $r \rightarrow +\infty$, given the asymptotic flatness of the space-time, implies that the energy of the particle is $E = m$. Further we will consider the energy and angular momentum per unit mass, thus replacing E and L with E/m and L/m so that the expression for the center of mass energy per unit mass becomes

$$\frac{E_{\text{cm}}^2}{2} = 1 + \frac{1}{F} - \frac{F L_1 L_2}{\Delta r^2} - \frac{1}{F} \sqrt{1 - F - \frac{F^2 L_1^2}{\Delta r^2}} \sqrt{1 - F - \frac{F^2 L_2^2}{\Delta r^2}}. \quad (22)$$

This expression depends on Δ and involves only on one metric function, F defining which solution we are describing. In the case of Schwarzschild (i.e. for $F = \Delta$) we retrieve the result obtained in [32] for which the center of mass energy at the horizon is finite and is given by

$$\lim_{r \rightarrow 2M} E_{\text{cm}}^{q=0} = \lim_{r \rightarrow 2M} E_{\text{cm}}^{\gamma=1} = \frac{\sqrt{L_1^2 - 2L_1L_2 + L_2^2 + 16M^2}}{2M}. \quad (23)$$

On the other hand, for both the ER and ZV metrics we obtain that E_{cm} diverges for prolate sources (i.e. $q > 0$ for ER and $\gamma < 1$ for ZV, respectively)

$$\lim_{r \rightarrow 2M} E_{\text{cm}}^{q>0} = \lim_{r \rightarrow 2M} E_{\text{cm}}^{\gamma<1} = +\infty. \quad (24)$$

For oblate sources (i.e. $q < 0$ for ER and $\gamma > 1$ for ZV), the center of mass energy tends to a minimum value that is independent of the value of the quadrupole moment

$$\lim_{r \rightarrow 2M} E_{\text{cm}}^{q<0} = \lim_{r \rightarrow 2M} E_{\text{cm}}^{\gamma>1} = 2. \quad (25)$$

However, it must be noted that $E_{\text{cm}}(r)$ for oblate sources approaches the minimum value at $r = 2M$ with vertical tangent (i.e. diverging first derivative) and thus also in this case the center of mass energy is not defined for $r < 2M$. The behaviour of E_{cm} as a function of r in the ER metric for different values of q is illustrated in the left panel of figure 1, while the corresponding behaviour in the ZV metric for different values of γ is illustrated in the right panel of figure 1.

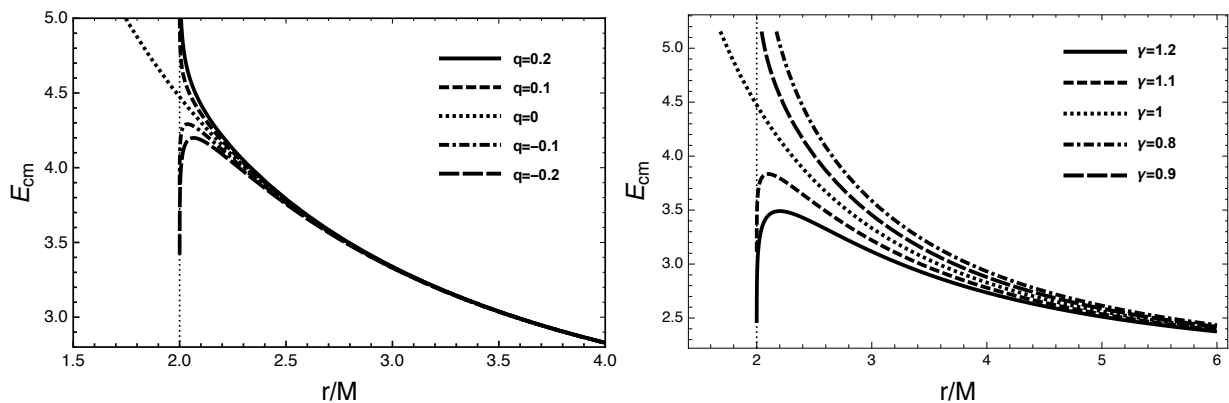


FIG. 1: The center of mass energy for the collision of two particles with given angular momentum $L_1 = -L_2 = 4$ in the ER space-time (left panel) and in the ZV space-time (right panel). The Schwarzschild case is retrieved for $q = 0$ in the ER metric and $\gamma = 1$ in the ZV metric.

It is important to notice here that not all possible orbits may occur around astrophysical compact objects. In fact collisions in the vicinity of the infinitely red-shifted surface may be extremely rare. However, there are several configurations that may be of interest, in particular, the ones involving particles on circular orbits. In general, circular orbits are not allowed in the vicinity of $r = 2M$ and it is important to distinguish the region where stable circular orbits can occur from the region where circular orbits are unstable. In the following we will consider two simple models for collisions:

- (A) Collision between two particles on circular orbits. In this case we consider two particles on circular orbit, i.e. $\dot{r}_1 = \dot{r}_2 = 0$, with the same value of $r_1 = r_2 = r$ and opposite angular momentum $L_1 = -L_2 = L$.
- (B) Collision between one particle on circular orbit and one particle on radial infall from infinity. In this case we consider one particle on circular orbit, i.e. $\dot{r}_1 = 0$ at a radius $r_1 = r$ with angular momentum $L_1 = L$ and one particle on radial trajectory $r_2(\tau)$ with $L_2 = 0$.

In figure 2 we show the center of mass energies for the above collisions in the ER metric, while figure 3 shows the corresponding energies for the ZV metric. Notice that for a given radius, the collision of two particles on circular orbits with opposite angular momentum produces more energy with respect to the collision of one particle on circular orbit with a particle infalling from infinity.

From the point of view of astrophysics we know that compact objects are generically accompanied by accretion disks of gas falling onto them. The trajectories of particles in the accretion disk can be described as circular geodesics. However, as said, for black holes and extremely collapsed objects particles can not exist on stable circular orbits arbitrarily close to the horizon or the surface of the object. The innermost stable circular orbit (ISCO) is a common tool to probe the behaviour test particles

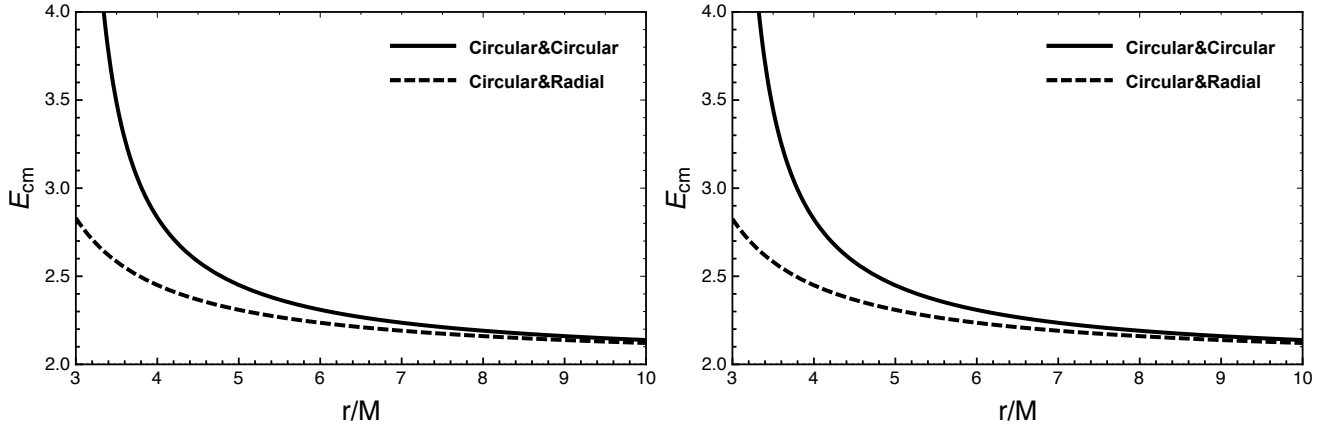


FIG. 2: Collision of particles in the ER space-time. Solid lines represent both particles on circular orbits; dashed lines represent one particle is on circular orbits and one particle falling radially from infinity. Left panel: Oblate case ($q = -0.1$). Right panel: Prolate case ($q = 0.1$).

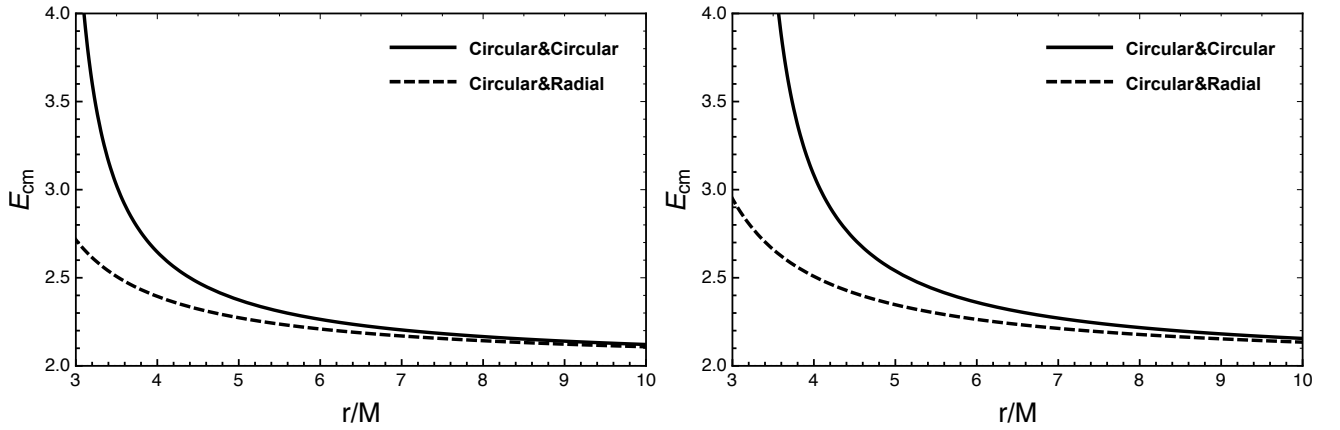


FIG. 3: Collision of particles in the ZV space-time. Solid lines represent both particles on circular orbits; dashed lines represent one particle is on circular orbits and one particle falling radially from infinity. Left panel: Prolate case ($\gamma = 0.9$). Right panel: Oblate case ($\gamma = 1.1$).

in accretion disks near compact objects. In the case of Schwarzschild the ISCO is located at $r_{isco} = 6M$, while unstable and unbound circular orbits can extend at most until $r = 3M$. On the other hand for the ER and ZV metric particles can exist on stable circular orbits closer or farther from the source based on the value of the quadrupole moment. For a metric of Weyl's class, the effective potential for a particle on circular orbit in the equatorial plane is obtained from equation (20) setting $\dot{r} = 0$ and it is given by

$$U_{eff} = \frac{F^2 L^2}{\Delta r^2} + F. \quad (26)$$

The condition for the particle to be on circular orbit is then given by $U'_{eff} = 0$, where the prime denotes derivatives with respect to r . The energy E , angular momentum L and angular velocity Ω per unit mass for particles on circular orbits can be also obtained from

$$E^2 = -\frac{g_{tt}^2}{g_{tt} + g_{\phi\phi}\Omega^2}, \quad (27)$$

$$L^2 = -\frac{g_{\phi\phi}^2 \Omega^2}{g_{tt} + g_{\phi\phi}\Omega^2}, \quad (28)$$

$$\Omega^2 = -\frac{g_{tt,r}}{g_{\phi\phi,r}}, \quad (29)$$

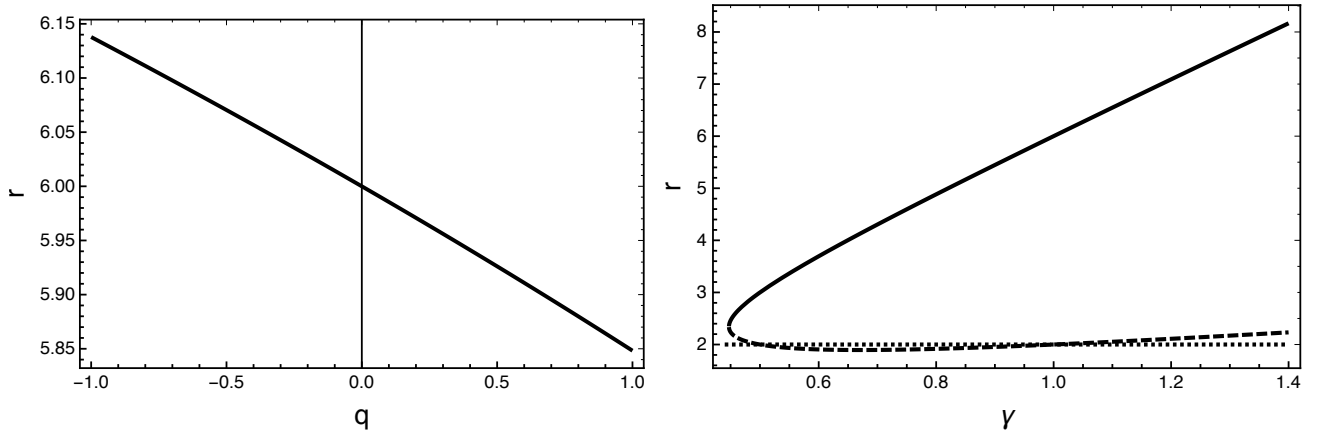


FIG. 4: The dependence of the ISCO radius on the deformation parameters q for ER metric (left panel) and γ for ZV metric (right panel).

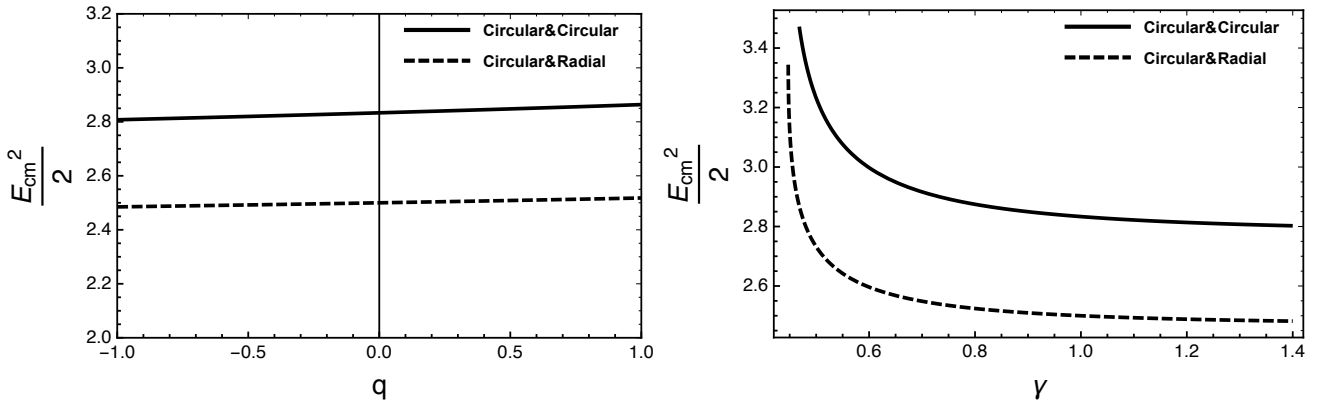


FIG. 5: The center of mass energy $E_{cm}^2/2$ for collisions at the ISCO of two particles on circular orbits (solid line) and one particle on circular orbit vs. one particle on radial infall (dashed line) as a function of q in the ER metric (left panel) and as a function of γ in the ZV metric (right panel).

and so, for metrics of Weyl's class, we can rewrite E and L for particles on circular orbit as

$$E^2 = \frac{F^2 L^2}{\Delta r^2} + F, \quad (30)$$

$$L^2 = \frac{F' \Delta^2 r^3}{F^2 (\Delta' r + 2\Delta) - 2F' F \Delta r}. \quad (31)$$

The radius of the ISCO is then given by the condition of marginal stability of the orbit, i.e. $U''_{eff} = 0$. For the ER metric the explicit form of r_{isco} is rather complicated, and it is given by the solution of the following implicit function:

$$H(r, q) = r - 6 + qr\Psi'(3r^2 - 18r + 28) + qr^2\Psi''(r - 2)(r - 1) - 6q^2r^2\Psi'^2(r - 2)(r - 3) + 4q^3r^3\Psi'^3(r - 2)^2 = 0, \quad (32)$$

where for simplicity we have replaced $r \rightarrow r/M$ and where $\Psi(r)$ is given by equation (9) with $\theta = \pi/2$. On the other hand, for the ZV metric the ISCO radius is simply given by

$$r_{isco} = M(1 + 3\gamma \pm \sqrt{5\gamma^2 - 1}). \quad (33)$$

Notice that there are two allowed values of $r_{isco} > 2M$ for $\gamma \in (1/\sqrt{5}, 1/2)$. In the following we will consider only the outer radius of the ISCO thus restricting the attention to the solution with plus sign in equation (33). In figure 4 we show the value of r_{isco} in the ER and ZV metrics as functions of q and γ respectively. A word of caution must be added regarding the interpretation of the parameters q and γ in relation to physical observables. For values of $q \simeq 0$ and $\gamma \simeq 1$ we can confidently describe small departures from spherical symmetry. On the other hand, for larger values, the contribution of the quadrupole moment (or higher multipole moments in the case of the ZV metric) may become dominant over the mass monopole, and this

may in turn affect the behavior of the orbits. For example, in the ZV metric, where monopole and the quadrupole moments contain both M and γ (see equations (16) and (17)), rewriting the equation for r_{isco} in terms of M_0 and M_2 shows that there is a limiting value $M_2 = 4M_0^3/3$ at which the contributions of the quadrupole moment produce substantial departures from the Schwarzschild-like behavior. A similar situation occurs in the ER metric where M_2 depends on both q and M .

We now wish to evaluate the center of mass energy for particles on the accretion disk at the ISCO as a function of the deformation parameters q and γ . In particular we shall restrict to the outer ISCO radius, which is the relevant case for astrophysical accretion disks. To obtain the value of the center of mass energy for collision of two particles on circular orbits at the ISCO we use equation (22) with $\dot{r}_1 = \dot{r}_2 = 0$ and $L_1 = -L_2 = L$ given by equation (31). The value of r_{isco} is obtained from $U''_{eff} = 0$. We then get

$$\frac{(E_{cm}^{cc})^2}{2} = 1 + \frac{1}{F} + \frac{F L^2}{\Delta r^2}, \quad (34)$$

where the superscript ‘cc’ stands for ‘circular-circular’. Similarly, to obtain the center of mass energy for the collision between one particle on circular orbit at the ISCO and one on radial infall from infinity, we use equation (22) with $\dot{r}_1 = 0$ and $L_2 = 0$. We obtain

$$\frac{(E_{cm}^{cr})^2}{2} = 1 + \frac{1}{F}, \quad (35)$$

where the superscript ‘cr’ stands for ‘circular-radial’.

In the case of the ER metric the form of E_{cm} at the ISCO for the two cases is rather complicated due to the fact that the ISCO is defined via the implicit function (32). In the left panel of figure 5 we show the center of mass energy for collision of two particles at the ISCO in the ER metric in the case of both particles on circular orbits with opposite angular momentum (‘cc’) and one particle on circular orbit and one particle radially falling from infinity (‘cr’).

In the case of the ZV metric E_{cm} at the ISCO for the two kinds of collisions can be evaluated explicitly and it becomes

$$\frac{(E_{cm}^{cc})^2}{2} = 1 + \left(\frac{3\gamma + 1 + \sqrt{5\gamma^2 - 1}}{3\gamma - 1 + \sqrt{5\gamma^2 - 1}} \right)^\gamma + \frac{\gamma}{\gamma + \sqrt{5\gamma^2 - 1}}, \quad (36)$$

$$\frac{(E_{cm}^{cr})^2}{2} = 1 + \left(\frac{3\gamma + 1 + \sqrt{5\gamma^2 - 1}}{3\gamma - 1 + \sqrt{5\gamma^2 - 1}} \right)^\gamma. \quad (37)$$

It is easy to notice that the center of mass energy at the ISCO is greater than zero and finite for all values of γ and it is greatest for the limiting case $\gamma = 1/\sqrt{5}$ while it tends to the smallest value for $\gamma \rightarrow +\infty$. We have the following limits

$$\lim_{\gamma \rightarrow 1/\sqrt{5}} \frac{(E_{cm}^{cc})^2}{2} = 2 + \left(\frac{3 + \sqrt{5}}{3 - \sqrt{5}} \right)^{1/\sqrt{5}}, \quad (38)$$

$$\lim_{\gamma \rightarrow 1/\sqrt{5}} \frac{(E_{cm}^{cr})^2}{2} = 1 + \left(\frac{3 + \sqrt{5}}{3 - \sqrt{5}} \right)^{1/\sqrt{5}}, \quad (39)$$

and

$$\lim_{\gamma \rightarrow +\infty} \frac{(E_{cm}^{cc})^2}{2} = \frac{2 + \sqrt{5}}{1 + \sqrt{5}}, \quad (40)$$

$$\lim_{\gamma \rightarrow +\infty} \frac{(E_{cm}^{cr})^2}{2} = 1. \quad (41)$$

It is also worth noticing that although the above limits for $\gamma \rightarrow 1/\sqrt{5}$ are finite the function $f(\gamma)$ given by $E_{cm}^2/2$ evaluated at r_{isco} approaches the limit with infinite tangent in both cases, i.e. $df/d\gamma \rightarrow +\infty$ for $\gamma \rightarrow 1/\sqrt{5}$. The center of mass energies for the two scenarios in the ZV metric are shown in the right panel of figure 5.

The difference between the same scenarios in the ER metric with respect to the ZV metric is due to the fact that the ER metric describes the contribution of the quadrupole moment for every value of q while for the ZV metric the contribution due to higher multipole moments becomes important for values of γ not close to unity.

IV. DISCUSSION

We considered the collision of test particles in the gravitational field of black hole mimickers described by exact solution of the vacuum Einstein's field equations with non vanishing quadrupole moment. We showed that, with the exception of the special case of spherical symmetry (i.e. Schwarzschild) the center of mass energy for collisions is defined only outside the infinitely red-shifted surface $r = 2M$. Under the assumption that exotic compact sources with quadrupole moment may exist in nature, our results show that particle collisions in close proximity of the surface of prolate objects may produce arbitrarily high energies. However, the collision energy at the innermost stable circular orbit is finite for both oblate and prolate objects and depends strongly on the value of the quadrupole moment. Therefore, at least in principle, such collisions could be used as a way to distinguish these kinds of exotic sources from black holes and thus test the possibility of existence of extreme compact objects with quadrupole moment in the universe.

Acknowledgement

The work was supported by Nazarbayev University Faculty Development Competitive Research Grant No. 090118FD5348 and by the Ministry of Education and Science of the Republic of Kazakhstan target program IRN: BR05236454.

-
- [1] W. Israel, *Phys. Rev.* **164**, 1776 (1967).
 - [2] B. Carter, *Phys. Rev. Lett.* **26**, 331 (1971).
 - [3] N. Gürlebeck, *Phys. Rev. Lett.* **114** (15), 151102 (2015).
 - [4] L. Herrera, *Int. J. Mod. Phys. D* **17**, 557 (2008).
 - [5] W. B. Bonnor, *Gen. Relat. Gravit.* **24**, 551 (1992).
 - [6] H. Weyl, *Ann. Phys.* **54**, 117 (1917).
 - [7] H. Weyl, *Ann. Phys.* **59**, 185 (1919).
 - [8] H. Quevedo, *Fortschr. Phys.* **58**, 10, 733 (1990).
 - [9] J. L. Hernandez-Pastora and J. Martin, *Gen. Relat. Gravit.* **26**, 877 (1994).
 - [10] R. Penrose, *Phys. Rev. Lett.* **14**, 57 (1965).
 - [11] S. Hawking and R. Penrose, *Proc. Roy. Soc. Lond. A* **A314**, 529 (1970).
 - [12] P. Chen, Y. C. Ong and D.-h. Yeom, *Phys. Rep.* **603**, 1 (2015).
 - [13] D. Malafarina, *Universe* **3** (2), 48 (2017).
 - [14] G. Erez and N. Rosen, *Bull. Res. Council Israel* 8F 47 (1959).
 - [15] A. Armenti, *Int. J. Theor. Phys.* **16** (11), 813 (1977).
 - [16] D. Bini, M. Crosta, F. de Felice, A. Geralico and A. Vecchiato, *Class. Quantum Grav.* **30**, 045009 (2013).
 - [17] H. Quevedo and L. Parker, *Gen. Relat. Gravit.* **23**, 495 (1991).
 - [18] K. Boshkayev, H. Quevedo, G. Nurbakyt, A. Malybayev and A. Urazalina, *Symmetry*, **11** (10), 1324 (2019).
 - [19] D. M. Zipoy *Journ. Math. Phys.* **22**, 1137 (1970).
 - [20] B. H. Voorhees, *Phys. Rev. D* **2**, 2119 (1970).
 - [21] D. Papadopoulos, B. Stewart and L. Witten, *Phys. Rev. D* **24**, 320 (1981).
 - [22] L. Herrera, F. M. Paiva and N. Santos, *Int. J. Mod. Phys. D* **9**, 649 (2000).
 - [23] A. N. Chowdhury, M. Patil, D. Malafarina and P. S. Joshi, *Phys. Rev. D* **85**, 104031 (2012).
 - [24] K. Boshkayev, E. Gasperin, A. Gutierrez-Pineres, H. Quevedo and S. Toktarbay, *Phys. Rev. D* **93** (2), 024024 (2016).
 - [25] C. A. Benavides-Gallego, A. Abdujabbarov, D. Malafarina, B. Ahmedov and C. Bambi, *Phys. Rev. D* **99** (4), 044012 (2019).
 - [26] A. B. Abdikamalov, A. A. Abdujabbarov, D. Ayzenberg, D. Malafarina, C. Bambi and B. Ahmedov, *Phys. Rev. D* **100** (2), 024014 (2019).
 - [27] B. Toshmatov, D. Malafarina and N. Dadhich, *Phys. Rev. D* **100** (4), 044001 (2019).
 - [28] B. Toshmatov and D. Malafarina, *Phys. Rev. D* **100** (10), 104052 (2019).
 - [29] L. Hernandez-Pastora and J. Martin, *Class. Quantum Grav.* **10**, 2581 (1993).
 - [30] Ts. I. Gutsunayev and V. S. Manko, *Gen. Relat. Gravit.* **17**, 1025 (1985).
 - [31] A. Armenti, *Celestial Mechanics* **6**, 383 (1972).
 - [32] M. Bañados, J. Silk and S. M. West, *Phys. Rev. Lett.* **103** (11), 111102 (2009).
 - [33] T. Jacobson and T. P. Sotiriou, *Phys. Rev. Lett.* **104** (2), 021101 (2010).
 - [34] T. Harada and M. Kimura, *Phys. Rev. D* **83** (2), 024002 (2011).
 - [35] O. B. Zaslavskii, *Phys. Rev. D* **82** (8), 083004 (2010).
 - [36] M. Kimura, K.-I. Nakao and H. Tagoshi, *Phys. Rev. D* **83** (4), 044013 (2011).
 - [37] M. Patil and P. S. Joshi, *Phys. Rev. D* **82** (10), 104049 (2010).
 - [38] M. Patil, P. S. Joshi and D. Malafarina, *Phys. Rev. D* **83** (6), 064007 (2011).
 - [39] H. E. J. Curzon, *Proc. London Math. Soc.* 23, 477 (1924).
 - [40] O. Semerák, T. Zellerin and M. Záček, *Mon. Not. R. Astron. Soc.* **308**, 691 (1999).